Multicomponent reaction-diffusion processes on complex networks

Sebastian Weber and Markus Porto
Institut für Festkörperphysik, Technische Universität Darmstadt, Hochschulstrasse 8, 64289 Darmstadt, Germany
(Received 9 May 2006; revised manuscript received 12 July 2006; published 11 October 2006)

We study the reaction-diffusion process $A+B\rightarrow\emptyset$ on uncorrelated scale-free networks analytically. By a mean-field ansatz we derive analytical expressions for the particle pair correlations and the particle density. Expressing the time evolution of the particle density in terms of the instantaneous particle pair correlations, we determine analytically the "jamming" effect which arises in the case of multicomponent, pairwise reactions. Comparing the relevant terms within the differential equation for the particle density, we find that the "jamming" effect diminishes in the long-time, low-density limit. This even holds true for the hubs of the network, despite that the hubs dynamically attract the particles.

DOI: 10.1103/PhysRevE.74.046108 PACS number(s): 89.75.Hc, 82.20.−w, 05.40.−a

I. INTRODUCTION

The merging of graph theory and methods from classical statistical physics has led to the modern theory of complex networks [1,2]. This development went along with the discovery of complex networks in a vast variety of sciences. Almost all observed real networks share a so-called scale-free degree distribution. That is, the number of links (the degree k) of a randomly chosen vertex of the network is distributed according to

$$P(k) \propto k^{-\gamma}. \tag{1}$$

For exponents $2<\gamma<3$ this distribution has a diverging second moment $\langle k^2\rangle$ for infinite size networks ($N\rightarrow\infty$). A very prominent example is the World Wide Web [3] with a value γ of approximately 2.1. As a consequence, the network is very robust against the removal of random nodes, but extremely weak upon removal of the highly connected nodes [4].

The diverging $\langle k^2\rangle$ leads to enormous fluctuations in the degree of a vertex and causes a large heterogeneity in the vertex connectivity. This crucial feature of scale-free networks has strong consequences on dynamical processes taking place on them. The absence of an epidemic threshold in the presence of a diverging $\langle k^2\rangle$ is one of the most notable examples [5,6].

A similar class of dynamical processes, the reaction-diffusion processes [7,8], has been studied numerically on networks by Gallos and Argyrakis [9,10] and shortly after also analytically within mean-field (MF) theory by Catanzaro *et al.* [11] (see Ref. [12] for a recent series-expansion approach to networks). This type of dynamics is capable of modeling epidemic spreading, chemical reactions, and many more. The analytical work by Catanzaro *et al.* calculated the density decay of the one component $A+A\rightarrow\emptyset$ reaction for homogeneous and heterogeneous complex networks. The results for homogeneous networks agree with the classical MF behavior of a density decay linear in time, $1/\rho^{(a)}(t)\propto t$. In the case of heterogeneous (i.e., scale-free) networks, one finds a more general power law for the density decay

$$\frac{1}{\rho^{(a)}(t)} \propto t^{\alpha(\gamma)}(\ln t)^{\beta(\gamma)}, \tag{2}$$

with the γ-dependent characteristic exponents given by

$$\alpha(\gamma) = \begin{cases} 1/(\gamma-2), & 2<\gamma<3, \\ 1, & \gamma\geq 3 \end{cases} \tag{3}$$

and

$$\beta(\gamma) = \begin{cases} 1, & \gamma=3, \\ 0, & \text{otherwise}. \end{cases} \tag{4}$$

The reason for this extremely fast density decay originates in the existence of a few vertices with a very large degree (so-called hubs) in a scale-free network. As the analysis shows, the density is constantly $1/2$ for vertices with a degree $k>k_c=\langle k\rangle/2\rho^{(a)}(t)$.

If one wants to extend these results to more complicated diffusion-annihilation dynamics, for instance, the $A+B\rightarrow\emptyset$ process, which up to now has been studied only numerically [9,10], one realizes that this diffusion-annihilation dynamics introduces forbidden diffusion steps, since a vertex can hold at most one particle at a time. This constraint prohibits an A (B) particle to diffuse to an adjacent vertex which is already occupied by another A (B) particle. As we are going to discuss below, this leads to a "jamming" effect, a new feature of the dynamical process. Nevertheless, the obtained solution has a structure similar to that of the $A+A\rightarrow\emptyset$ process. The paper begins in Sec. II with a MF calculation of the particle pair correlations in dependence of the particle density. It follows a MF ansatz for the density decay of the $A+B\rightarrow\emptyset$ process from which we quantify the "jamming" effect. The results of the analytical work are compared with numerical simulations in Sec. III. At last, we conclude with Sec. IV.

II. THE $A+B\rightarrow\emptyset$ REACTION ON COMPLEX NETWORKS

We assume the complex network of N nodes to be fully defined by its $N\times N$ adjacency matrix a_{ij}. To discuss a physically meaningful complex network in the sense of diffusion, we take the network to be undirected and free of self- and multiple-connections. Therefore, a_{ij} is a traceless, symmetric

binary matrix with the elements a_{ij} being 0 or 1, which symbols a (dis)connection between site i and j. The state of vertex i at time t is described by two dichotomous variables $n_i^{(a)}(t)$ and $n_i^{(b)}(t)$. Their values may be 1 or 0 only, indicating the presence or absence of a particle A $[n_i^{(a)}(t)]$ and B $[n_i^{(b)}(t)]$.The system state is thus defined by

$$\mathbf{n}(t) = \mathbf{n}^{(a)}(t) + \mathbf{n}^{(b)}(t)$$

$$\mathbf{n}^{(a)}(t) = \{n_1^{(a)}(t), n_2^{(a)}(t), \ldots, n_N^{(a)}(t)\}$$

$$\mathbf{n}^{(b)}(t) = \{n_1^{(b)}(t), n_2^{(b)}(t), \ldots, n_N^{(b)}(t)\}. \quad (5)$$

Note that these variables have to fulfill the constraint $n_i^{(a)}(t)n_i^{(b)}(t)=0$ at any time. In the course of the calculation, we will take the average over multiple realizations of the same system, turning the discrete $n_i^{(a)}(t)$ and $n_i^{(b)}(t)$ variables into densities $\rho_i^{(a)}(t)$ and $\rho_i^{(b)}(t)$. Furthermore, we will assume throughout the analysis the statistical equivalence of vertices of the same degree k. Therefore, denoting by $\mathcal{V}(k)$ the set of all vertices with the same degree k, we assume that

$$\rho_i^{(a)}(t) \equiv \rho_k^{(a)}(t), \quad \forall\, i \in \mathcal{V}(k),$$

$$\rho_i^{(b)}(t) \equiv \rho_k^{(b)}(t), \quad \forall\, i \in \mathcal{V}(k) \quad (6)$$

is valid. Following standard MF treatment, we hence neglect all fluctuations which might exist within a set of vertices $\mathcal{V}(k)$. The total density $\rho^{(a)}(t)$ $[\rho^{(b)}(t)]$ is given by the set of partial particle densities $\{\rho_k^{(a)}(t)\}$ $(\{\rho_k^{(b)}(t)\})$ through the relation

$$\rho^{(a)}(t) = \sum_k \rho_k^{(a)}(t)P(k). \quad (7)$$

A dynamics starts by random assignment of maximal one particle per vertex. The particles diffuse by random jumps at a rate λ to adjacent neighbors through the network. If two different particles meet at a vertex, they instantly annihilate and the vertex becomes empty. Before we proceed to the time evolution of the system, we first derive an expression for the particle pair correlations in dependence of the partial particle densities.

A. Particle pair correlations

We quantify the particle pair correlations for given partial particle densities by counting the number of contacts between particles on adjacent vertices. To count the AB contacts of a vertex i, we assume vertex i to carry an A particle and count the number of adjacent vertices which are occupied by a B particle. Setting this number in relation to all connections of the vertex i yields the pair-correlation coefficient

$$q_i^{(ab)}(t) = \frac{1}{k_i} n_i^{(a)}(t) \sum_j a_{ij} n_j^{(b)}. \quad (8)$$

Averaging now over a whole ensemble of equal systems and making use of the usual MF assumption $\langle n_i^{(a)}(t)n_j^{(b)}(t)\rangle \approx \langle n_i^{(a)}(t)\rangle\langle n_j^{(b)}(t)\rangle$, we obtain

$$Q_i^{(ab)}(t) = \frac{1}{k_i}\rho_i^{(a)}(t)\sum_j a_{ij}\rho_j^{(b)}(t). \quad (9)$$

By using the statistical equivalence of all N_k vertices i with the same degree k, we can sum over all these vertices such that

$$Q_k^{(ab)}(t) = \frac{1}{k}\rho_k^{(a)}\sum_{k'} \rho_{k'}^{(b)}(t)\frac{1}{N_k}\sum_{i\in\mathcal{V}(k)}\sum_{j\in\mathcal{V}(k')} a_{ij}. \quad (10)$$

In this step, we split the sum with index j into two sums over k' and one over $\mathcal{V}(k')$. The double sum over a_{ij} is related to the conditional probability $P(k'|k)$ that a vertex of given degree k has a neighbor which has degree k'. This equation has been derived previously [6] to be

$$\frac{1}{kN_k}\sum_{i\in\mathcal{V}(k)}\sum_{j\in\mathcal{V}(k')} a_{ij} = P(k'|k). \quad (11)$$

Using this equation and assuming an uncorrelated network, which simplifies the conditional probability $P(k'|k)$ to $k'P(k')/\langle k\rangle$, we obtain the expression

$$Q_k^{(ab)}(t) = \rho_k^{(a)}(t)\Theta^{(b)}(t), \quad (12)$$

where we define

$$\Theta^{(b)}(t) = \frac{1}{\langle k\rangle}\sum_{k'} k'\rho_{k'}^{(b)}(t)P(k'). \quad (13)$$

One should note that by introducing the mean $\langle k\rangle$, the values of the exponent γ are limited to $\gamma>2$. Otherwise the mean $\langle k\rangle$ is not defined in the limit of infinite size networks $(N\to\infty)$. The overall particle pair-correlation coefficient $Q^{(ab)}(t)$ can easily be computed by multiplying Eq. (12) with $P(k)$ and summing once more over all k,

$$Q^{(ab)}(t) = \rho^{(a)}(t)\Theta^{(b)}(t). \quad (14)$$

Analogously, we have $Q^{(aa)}(t)=\rho^{(a)}(t)\Theta^{(a)}(t)$, $Q^{(bb)}(t)=\rho^{(b)}(t)\Theta^{(b)}(t)$, and $Q^{(ba)}(t)=\rho^{(b)}(t)\Theta^{(a)}(t)$.

B. Density decay

For further computations we will assume for simplicity that the initial densities of $\rho^{(a)}$ and $\rho^{(b)}$ are equal, so that there is a symmetry between A and B particles. We will calculate only an expression for $n^{(a)}(t)$, and one may obtain the corresponding $n^{(b)}(t)$ equations by interchanging indices A and B. Modeling the diffusion as a Poisson process [13], the set of $\{n_i^{(a)}(t)\}$ changes within an infinitesimal time interval dt as

$$n_i^{(a)}(t+dt) = n_i^{(a)}(t)\,\eta_i^{(a)}(dt) + \{1-[n_i^{(a)}(t)+n_i^{(b)}(t)]\}\xi_i^{(a)}(dt). \quad (15)$$

Here $\eta_i^{(a)}$ and $\xi_i^{(a)}$ are dichotomous random variables, taking values of 0 or 1 with certain probabilities p and $1-p$, respectively,

$$\eta_i^{(a)}(dt) = \begin{cases} 0, & p = \lambda dt \left[\sum_j \frac{a_{ij} n_j^{(b)}(t)}{k_j} + \left(1 - \frac{1}{k_i} \sum_j a_{ij} n_j^{(a)}(t) \right) \right], \\ 1, & 1 - p, \end{cases} \tag{16}$$

$$\xi_i^{(a)}(dt) = \begin{cases} 1, & p = \lambda dt \sum_j \frac{a_{ij} n_j^{(a)}(t)}{k_j}, \\ 0, & 1 - p. \end{cases} \tag{17}$$

The following two cases need to be distinguished. (i) If site i is occupied by an A particle at instant t, $\eta_i^{(a)}(dt)$ is responsible for the next time step: The site may become empty ($\eta_i^{(a)}=0$) with a probability proportional to the product of the jumping rate λ and the time interval dt if a B particle in the neighborhood jumps onto site i or if the A particle at i jumps away to a neighborhood site where no A particle is already located. Otherwise no change happens. (ii) If the site i is empty at instant t, then $\xi_i^{(a)}(dt)$ will determine the time evolution: The vertex may become occupied by an A particle only if one in the neighborhood jumps onto vertex i. Note that the two random variables $\eta_i^{(a)}$and $\xi_i^{(a)}$ are hence not independent from each other, but we will treat them as independent (see Ref. [11]).

Equation (15) yields an average time evolution for $n_i^{(a)}(t)$

$$\langle n_i^{(a)}(t+dt)\rangle = n_i^{(a)}(t) - dt \left\{ n_i^{(a)}(t) + \sum_j \left[n_i^{(a)}(t) \frac{a_{ij} n_j^{(b)}(t)}{k_j} - n_i^{(a)}(t) \frac{1}{k_i} a_{ij} n_j^{(a)}(t) - \left(1 - \left[n_i^{(a)}(t) + n_i^{(b)}(t) \right] \right) \frac{a_{ij} n_j^{(a)}(t)}{k_j} \right] \right\}, \tag{18}$$

where we have set without loss of generality the jumping rate $\lambda=1$. Averaging over a whole set of equal initial configurations and applying once more Eq. (11) and the statistical equivalence of vertices with the same degree, Eq. (6), we obtain after some formal rearrangements

$$\frac{d\rho_k^{(a)}}{dt} = -\rho_k^{(a)} - \sum_{k'} \left\{ \frac{1}{k'} \left[\rho_k^{(a)} \rho_{k'}^{(b)} - k' \rho_k^{(a)} \frac{1}{k} \rho_{k'}^{(a)} - \rho_{k'}^{(a)} + \rho_k^{(a)} \rho_{k'}^{(a)} + \rho_k^{(b)} \rho_{k'}^{(a)} \right] k P(k'|k) \right\}. \tag{19}$$

Here we have suppressed the explicit time dependence for the sake of simplicity. Assuming the network to be uncorrelated [i.e., that $P(k'|k)=k' P(k')/\langle k\rangle$] allows us to perform the sum over k', yielding finally the expression

$$\frac{d\rho_k^{(a)}}{dt} = -\rho_k^{(a)} - \frac{k}{\langle k\rangle} \left[\rho_k^{(a)} \rho^{(b)} - \rho^{(a)} + \rho_k^{(a)} \rho^{(a)} + \rho_k^{(b)} \rho^{(a)} \right] + \rho_k^{(a)} \Theta^{(a)} \tag{20}$$

for the partial particle densities. Multiplying Eq. (20) with $P(k)$ and summing over all k values results in the differential equation for the overall density

$$\frac{d\rho^{(a)}}{dt} = -\rho^{(b)} \Theta^{(a)} - \rho^{(a)} \Theta^{(b)} = -Q^{(ab)} - Q^{(ba)}. \tag{21}$$

From Eq. (21) it is apparent that the density decay is directly proportional to the pair correlations among unlike particles. To proceed further, we need expressions for $\rho_k^{(a)}$ and $\rho_k^{(b)}$. Since the initial densities are equal, we have forcibly $Q^{(aa)}=Q^{(bb)}$ because of symmetry. This implies the equality $\rho_k^{(a)}=\rho_k^{(b)}\equiv\rho_k'$, allowing further simplifications and transforming Eq. (20) into

$$\frac{d\rho_k'}{dt} = -\rho_k' + \frac{k}{\langle k\rangle} [1 - 3\rho_k'] \rho' + \rho_k' \Theta' = -\rho_k' + \frac{k}{\langle k\rangle} [1 - 3\rho_k'] \rho' + Q_k''. \tag{22}$$

This differential equation is very similar to the one previously found for the $A+A\to\varnothing$ process [11], with an additional term $Q_k''\equiv Q_k^{(aa)}=Q_k^{(bb)}$ and a coefficient of 3 instead of 2 in front of ρ_k'. The additional term measures the number of contacts among particles of the same type, which slow down the reaction as these jumps are prohibited, causing a "jamming" effect.

To test whether this new term $Q_k''=\rho_k'\Theta'$ alters the behavior of the dynamics, we compare it to the other term $3k\rho_k'\rho'/\langle k\rangle$, which is as well quadratic in the density, and find

$$\frac{\Theta'}{3\rho' k/\langle k\rangle} = \frac{1}{3k} \frac{\sum_{k'} k' \rho_{k'}' P(k')}{\sum_{k'} \rho_{k'}' P(k')} = \frac{1}{3k} \frac{\langle k' \rho_{k'}'\rangle}{\langle \rho_{k'}'\rangle}. \tag{23}$$

Due to the fact that the particles are dynamically attracted by the hubs of the network, which has been shown analytically in Ref. [11] for the $A+A\to\varnothing$ process and numerically for the $A+B\to\varnothing$ process in Ref. [9] as well, we propose the following approximation to proceed: We know from the $A+A\to\varnothing$ process that hubs ($k>k_c$) drive the dynamics, and that the density on those hubs is almost constant $\rho_c=1/2$, whereas the density on vertices which are not hubs is substantially lower. If we approximate the densities of all vertices with a degree $k<k_c$ to be zero, the terms $\langle k'\rho_{k'}'\rangle$ and $\langle \rho_{k'}'\rangle$ become in the thermodynamic limit

$$\langle k\rho_k'\rangle \approx \rho_c' \sum_{k=k_c}^{\infty} kP(k) \approx \rho_c' \int_{k_c}^{\infty} k^{1-\gamma} dk = \rho_c' \frac{k_c^{2-\gamma}}{\gamma-2}, \quad (24)$$

$$\langle \rho_k'\rangle \approx \rho_c' \sum_{k=k_c}^{\infty} P(k) \approx \rho_c' \int_{k_c}^{\infty} k^{-\gamma} dk = \rho_c' \frac{k_c^{1-\gamma}}{\gamma-1}. \quad (25)$$

In this step, we apply the continuous k approximation, which allows us to replace the sum by an integral. By inserting expressions (24) and (25) into Eq. (23), we find

$$\frac{\Theta'}{3\rho' k/\langle k\rangle} \approx \frac{1}{3}\frac{\gamma-1}{\gamma-2}\frac{k_c}{k}. \quad (26)$$

Therefore, we can neglect Q_k'' for a vertex with $k \gg k_c$. For $k \ll k_c$, we can neglect Q_k'' (and $3k\rho_k'\rho'/\langle k\rangle$) as this term is quadratic in the density, being very small for nodes with $k \ll k_c$ in the long-time, low-density limit. The intermediate range of $k \approx k_c$ is difficult to assess analytically and needs to get quantified in the next section by numerical simulations, which show that expression (23) is substantially smaller than 1 in the low density limit even for the range where $k \approx k_c$. Therefore, "jamming" is only of relevance for vertices with a low degree and high densities.

The calculation leading to Eq. (26) is carried out in the limit of infinite size network. In all real networks, one inevitably has a maximum degree $k_{\max}$ inducing finite-size effects. This maximum degree $k_{\max}$ limits the upper bound of the integrals in Eqs. (24) and (25). Evaluating these integrals with such an upper bound, one obtains

$$\frac{\Theta'}{3\rho' k/\langle k\rangle} \approx \frac{1}{3}\frac{\gamma-1}{\gamma-2}\frac{k_c}{k} f(k_c/k_{\max}), \quad (27)$$

with

$$f(x) = \frac{1-x^{\gamma-2}}{1-x^{\gamma-1}}. \quad (28)$$

The scaling function $f(x)$ has the limiting values

$$f(x) = \begin{cases} 1, & x \to 0, \\ \dfrac{\gamma-2}{\gamma-1}, & x \to 1. \end{cases} \quad (29)$$

Since $f(x)$ is a monotonically decreasing function for $\gamma > 2$, the finite-size effect on the result in Eq. (26) is to slightly decrease the importance of the "jamming" term evenly for all degrees k.

Concluding that the "jamming" effect is not relevant in the long-time, low-density limit, we neglect the $Q_k'' = \rho_k' \Theta'$ term in Eq. (22) and obtain an equation which relates ρ_k' to its derivative. However, we aim at a relation for ρ_k' itself. As done for the $A+A \to \emptyset$ process [11], we proceed with the quasistatic approximation, setting $d\rho_k'/dt \approx 0$. This assumes that the diffusion process is at any time much faster than the annihilation reaction (see also Ref. [14]). This approximation should be valid in the case of low densities, when the complex network is sparsely populated and the number of diffusion events in a time interval dt is much larger than the annihilation events, implying that the particles are always in an equilibrium state with respect to the degree distribution. Doing so, we get an approximate expression for ρ_k',

$$\rho_k' = \frac{\rho' k/\langle k\rangle}{1 + 3\rho' k/\langle k\rangle}. \quad (30)$$

This expression for ρ_k' has the same structure as found for the $A+A \to \emptyset$ process except that the coefficient of ρ' in the denominator is 3 instead of 2. As the structure of the differential equations is the same as for the $A+A \to \emptyset$ process, we obtain the same scaling behavior of Eqs. (3) and (4) for each component. The new critical k_c for which a vertex is sensed as a hub by the dynamics is $k_c = \langle k\rangle/3\rho' = 2\langle k\rangle/3\rho$. Therefore, for the hubs in the system with $k > k_c$, Eq. (30) is close to 1/3, which is completely consistent with MF, as this means that hubs are occupied by approximately 1/3 of the time by each component A and B, and are empty for the remaining 1/3 of the time.

III. NUMERICAL SIMULATIONS

To test the analytical results obtained, we performed intensive numerical simulations of the $A+B \to \emptyset$ process on scale-free networks. The uncorrelated, scale-free networks are generated with the uncorrelated configuration model (UCM) algorithm [15–17] and have a size of $N = 10^6$ if not stated otherwise. The exponents γ simulated are in the range of 2.1 to 3.5, while we only present a suitable subset in the figures. In short, one draws for a network of size N a random number for each vertex according to the degree distribution $P(k) \propto k^{-\gamma}$, with an upper cutoff $k_{\max} = N^{1/2}$ to ensure that the generated network is uncorrelated [18]. The drawn number corresponds to the target degree of each node and can be understood as half edges to be joint with other half edges to form a connection. This is done in the central loop, in which one draws randomly two half edges and joins them if this neither creates a self-connection nor a multiple connection. Upon a successful join of two half-edges, these two half-edges are dropped from the set of eligible half-edges. In any case, one continues with the central loop by drawing again two half-edges, and so forth. After the distribution of all half-edges, we only keep the largest component of the generated network. We use a minimum degree of $k_{\min} = 2$ in our simulations, so that the largest component usually coincides with the full network. We have verified that the networks are indeed uncorrelated by obtaining the degree-degree correlation coefficient [19], which has an absolute value smaller than 10^{-3} in all cases. On these networks, the dynamics is simulated in the following way: Initially a fraction $\rho = 2\rho^{(a)} = 2\rho^{(b)}$ of randomly chosen vertices is selected, which we choose as $\rho = 0.1$ or 0.95. Then, the algorithm assigns randomly an equal amount of A and B particles to the set of chosen vertices. After this initial setup, the diffusion-annihilation dynamics starts. First, a vertex which carries a

particle and a random adjacent neighbor of this vertex are randomly selected. Three cases need to be distinguished: (i) If the neighbor vertex is empty, the particle moves to the new vertex, leaving the initial vertex empty. (ii) If the neighbor vertex is occupied by a particle of the other type, an annihilation reaction occurs and both vertices become empty. Accordingly, the number of particles is decreased for each particle type by one, $n^{(a)} \to n^{(a)} - 1$, and $n^{(b)} \to n^{(b)} - 1$. (iii) If the neighbor vertex is occupied by a particle of the same type, then no jump occurs. In any case, the time is updated by $t \to t + 1/(n^{(a)} + n^{(b)})$, where $n^{(a)}$ and $n^{(b)}$ correspond to the values before the diffusion step, and one continues by selecting randomly another vertex carrying a particle, and so forth.

In order to obtain the system's typical behavior, we average over 50 independent dynamics on each graph and over 100 independent graphs, making up a total of 5000 dynamics per data point.

A. Validation of the approximations

To validate the analytical calculations developed in the last section, we have to verify the two central approximations made which are based on the assumption of a small particle density on the network. Furthermore, it is crucial to get an estimate which densities can be considered small enough for the validity of the approximations. Our first approximation was to neglect in Eq. (20) the "jamming" term Q_k'' in comparison to the other term quadratic in the density $3k\rho_k'\rho'/\langle k\rangle$. We have shown the validity of this approximation analytically for vertices with a degree $k \gg k_c$ and $k \ll k_c$ (the latter for low densities). To check the intermediate range $k \approx k_c$, we perform numerical simulations. If we set the ratio in Eq. (23) equal to 1, we obtain a critical degree $\tilde{k}_c$,

$$\tilde{k}_c = \frac{\Theta'}{3\rho'/\langle k\rangle}, \tag{31}$$

which separates vertices whose "jamming" term is less important than the other quadratic density term in Eq. (22) from those vertices for which the "jamming" term is at least of equal importance. The time-evolution of the particle density on vertices with a degree $k \gg \tilde{k}_c$ is not affected by "jamming," whereas vertices with a degree of the order of $\tilde{k}_c$ or lower are affected. On the other hand vertices with a small degree do not contribute to the overall particle density at later times, since the hubs dynamically attract the particles and carry the highest density $\rho_c' = 1/3$. Considering only vertices as hubs which have a degree $k > k_c = \langle k\rangle/3\rho'$, we have as a condition for "jamming" not being relevant

$$\tilde{k}_c \ll k_c. \tag{32}$$

If condition (32) is fulfilled, there are no vertices left in the network which do carry a sufficiently high density and whose "jamming" term is important for the time-evolution of their $\rho_k(t)$. In Fig. 1 we exemplified this condition for an exponent $\gamma = 2.75$ and an initial particle density $\rho_0 = 0.95$. Note that the curves are only drawn until k_c reaches the value of the maximum degree $k_{\max}$ present in the network. Once

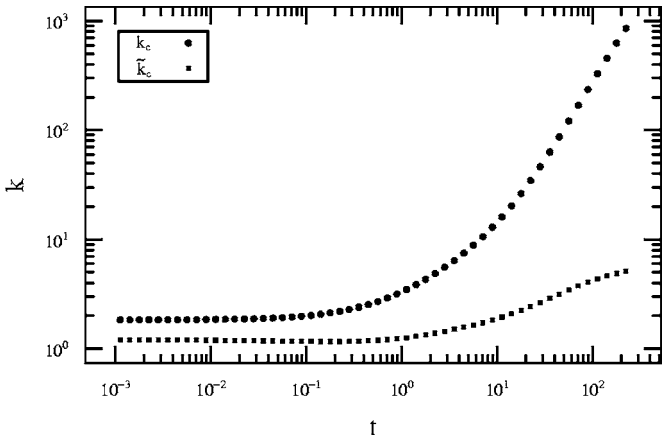

FIG. 1. Plot of k_c and $\tilde{k}_c$ of the numerically simulated $A+B \to \emptyset$ process for an exponent $\gamma = 2.75$ and an initial density $\rho_0 = 0.95$. Since k_c is increasing much faster than $\tilde{k}_c$, "jamming" becomes quickly irrelevant.

the value of k_c is much greater than $\tilde{k}_c$ the "jamming" effect is of no more relevance for the time evolution of the process for all vertices in the network, including those with $k \approx k_c$. It is crucial to note that k_c grows much faster than $\tilde{k}_c$ in the course of the process. Therefore, the "jamming" is continuously diminishing during the dynamics and only important for low degree vertices carrying a high density in the beginning of the process. An equivalent criterion to test whether "jamming" is not relevant is to check if the ratio of $\tilde{k}_c/k_c$ is substantially smaller than 1. In Fig. 2(a) we illustrate this for an initial density $\rho_0 = 0.95$. Again, the individual curves are only drawn until k_c reaches $k_{\max}$. They start with a maximum value of almost 1, indicating the presence of "jamming" and drop quite quickly well below 1. In Fig. 2(b) we show the same simulations starting but with a much smaller initial density of $\rho_0 = 0.1$. Most importantly, these curves already begin at values well below 1 and therefore there is never "jamming" present in the dynamics. The interesting intermediate increase of $\tilde{k}_c/k_c$ for the initial density $\rho_0 = 0.1$ [Fig. 2(b)] comes from the fact the dynamical hubs start with a density $\rho_0' = 0.05$ which is smaller than their long-time density $\rho_c' = 1/3$. Therefore, all vertices with $\rho_k' < 1/3$ and a degree $k > k_c$ will have increasing particle densities ρ_k' which enter Θ' in Eq. (31). Once the dynamics has reached its long-time behavior, there are no more ρ_k' terms in Θ' which increase in magnitude, since the dynamical hubs carry the highest density in the network.

The second approximation made to obtain an expression for ρ_k', the quasistatic assumption $d\rho_k^{(a)}/dt \approx 0$, yielded Eq. (30). Rearranging Eq. (30) into

$$k\left(\frac{1}{\rho_k'} - 3\right) = \frac{\langle k\rangle}{\rho'} \tag{33}$$

leads to an expression where the right hand side (and consequently the left hand side as well) is independent of k if the approximation is indeed valid. Plotting the left hand side of Eq. (33) for a couple different degrees k should yield a data

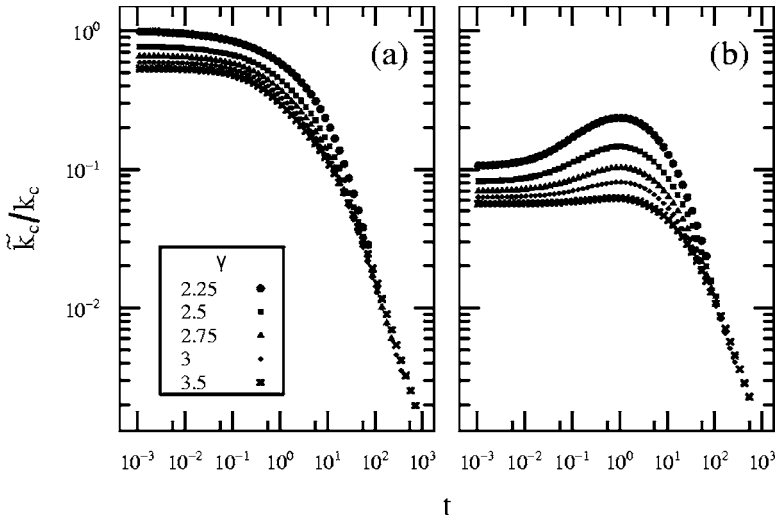

FIG. 2. Ratio of $\tilde{k}_c$ and k_c of the numerically simulated $A+B\to\emptyset$ process on networks of different exponents γ as indicated, with (a) an initial particle density $\rho_0=0.95$ and (b) $\rho_0=0.1$.

collapse onto a single curve. Figure 3 illustrates this in the case of an exponent $\gamma=2.5$. The curves join quite nicely at roughly $t\approx 50$. Similar time points are obtained for other exponents γ. We can therefore expect that the quasistatic approximation holds after this time.

B. Density decay and pair correlations

The verification of the scaling behavior for each component as predicted by Eqs. (3) and (4) turns out to be a hard numerical problem, as finite-size effects occur quite early. A detailed discussion and derivation of finite-size effects for the $A+A\to\emptyset$ process can be found in Ref. [11]. The typical "scale-free" behavior of the dynamics corresponds to a density decay as a power-law of the time with an exponent larger than 1. Catanzaro *et al.* [11] showed that the characteristic "scale-free" behavior of the dynamics is driven by the "dynamical" hubs of the system, where "dynamical" hubs are

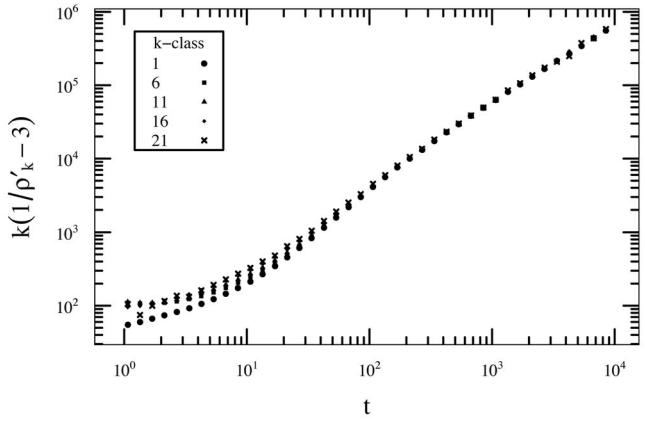

FIG. 3. Numerical validation of the quasistatic approximation according to Eq. (33) for the $A+B\to\emptyset$ process, exemplified by an exponent $\gamma=2.5$ and an initial density $\rho_0=0.1$. The k classes are logarithmically joined, where class 1 corresponds to vertices of degree $k=2$, class 6 to $8\leq k\leq 10$, class 11 to $33\leq k\leq 42$, class 16 to $134\leq k\leq 178$, and class 21 to $563\leq k\leq 750$. A data collapse is observed for $t\gtrsim 50$.

those vertices which have a degree $k>k_c\propto 1/\rho^{(a)}$. As the density is decreasing monotonically in time, the number of "dynamical" hubs decreases as well. Thus, if in a finite network of size N there are no "dynamical" hubs left, the density decay turns over to a decay linear in time. The vertex with the largest degree $k_{\max}$ therefore limits the duration until the crossover from "scale-free" to "non-scale-free" behavior happens. On the other hand, the largest degree $k_{\max}$ being possible for uncorrelated scale-free networks which contain neither self- nor multiple connections scales with the square root of the system size, $k_{\max}\propto N^{1/2}$, making very large system sizes necessary.

One might expect that the scaling exponent derived in MF theory for each component's density decay $\alpha(\gamma)=1/(\gamma-2)$, is missing some effects which slow down the reaction for exponents γ close to 2. Otherwise, the diverging $\alpha(\gamma)$ for $\gamma\to 2$ would result in a diverging reaction speed. Forcibly, we expect to recover the scaling law given by $\alpha(\gamma)$ for $\gamma\to 3$. Choosing a value of γ which is smaller than but close to 3 has the convenient side effect that the density decay is relatively slow, such that the dynamics will show a scale-free

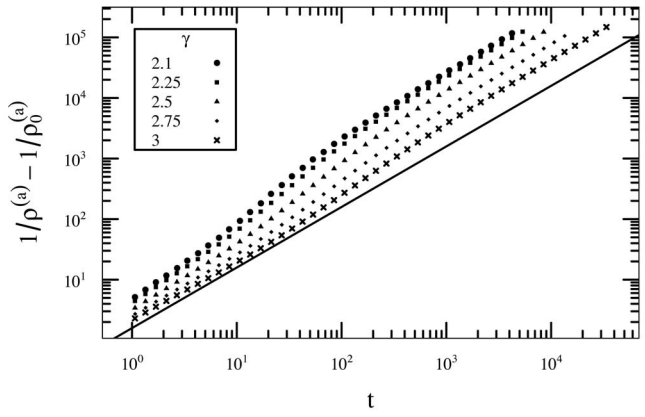

FIG. 4. Density decay of the numerically simulated $A+B\to\emptyset$ process for an initial density $\rho_0=0.1$ and different exponents γ. With increasing exponent γ, the density decay behaves "scale-free" typical for a longer period of time. The solid line has a slope of 1 and is shown as a guide to the eye.

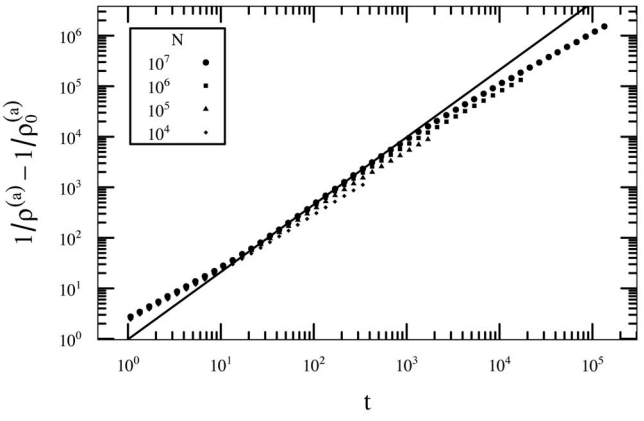

FIG. 5. Density decay of the numerically simulated $A+B\rightarrow\emptyset$ process for networks of various sizes, exemplified by an exponent $\gamma=2.75$ and an initial density $\rho_0=0.1$. The plot illustrates the strong finite-size effects of the dynamics. For $\gamma=2.75$ the process is sufficiently slow to show the theoretic slope of 4/3 (drawn as a solid line) for large networks with size $N=10^7$ for two decades.

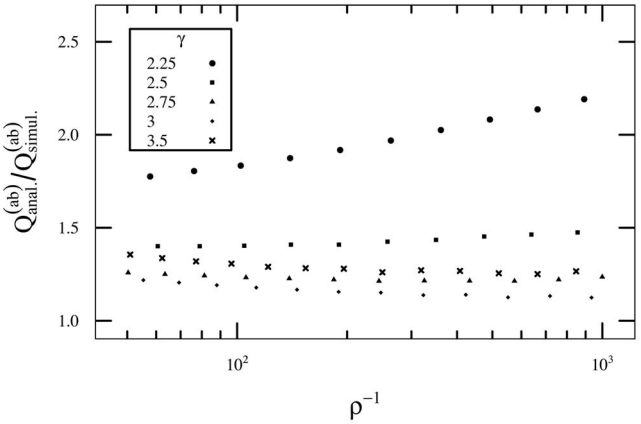

FIG. 6. Ratio between the analytically calculated correlations $Q_{\mathrm{anal}}^{(ab)}$ and the numerically obtained one $Q_{\mathrm{simul}}^{(ab)}$, plotted as a function of the inverse density ρ^{-1} for an initial density $\rho_0=0.1$ and different exponents γ. The range of the inverse density shown is limited by the validity of the quasistatic approximation, which is valid at sufficiently low densities $\rho^{-1}>5\times10^1$. However, the inverse density is also limited from above to $\rho^{-1}<10^3$, as the pair correlation is quadratic in the particle density. Such observables can only be meaningfully resolved as long as $\rho>N^{-1/2}$, which yields the condition $\rho>10^{-3}$ for the given system size of $N=10^6$.

behavior for a longer period of time with the appropriate density decay exponent larger than 1. We verify this assumption by simulating the $A+B\rightarrow\emptyset$ process for various exponents γ while keeping the system size constant at $N=10^6$. In Fig. 4 we show the resulting density decays. The curves deviate from a linear in time decay only for very short durations, but the amount of time with which each process behaves scale-free increases with increasing exponent γ. To recover the scaling behavior of $\rho^{(a)}$, we chose an exponent $\gamma=2.75$ which corresponds to a value $\alpha=4/3$. In Fig. 5, we present the results for the density decay $\rho^{(a)}$ for various network sizes of up to $N=10^7$. Nevertheless, even for a system size of $N=10^7$, the density decay shows scale-free behavior only for less than two decades.

A far more sensitive alternative check of the analytical calculations is given by the direct comparison of the analytically calculated particle pair correlations, Eq. (14), and the measured ones from numerical simulations, as these particle pair correlations directly drive the annihilation rate. Therefore, we evaluate the ratio between the analytical predictions of Eq. (14) and the corresponding numerically obtained values for the pair correlations. It is crucial to note that $Q^{(ab)}(t)$ can be understood as a function of all partial particle densities $\rho_k^{(a)}(t)$ and $\rho_k^{(b)}(t)$, so that it depends only implicitly via these densities on time t. Approximating these partial particle densities via the quasi-static assumption, one may write the particle pair correlations as a function of the inverse particle density ρ^{-1} by using Eq. (30),

$$Q_{\mathrm{anal}}^{(ab)}(\rho^{-1}) = \frac{1}{2\rho^{-1}}\frac{1}{\langle k\rangle}\sum_{k'} k'\frac{k'/\langle k\rangle}{2\rho^{-1}+3k'/\langle k\rangle}P(k'). \quad (34)$$

The inverse particle density ρ^{-1} can be regarded as an alternative measure of time, since ρ^{-1} is a monotonically increasing function in the course of the dynamics. In Fig. 6, we present the resulting ratios for various exponents γ. The expected value of 1 for the ratio, which would mean perfect agreement of analytical and numerical particle pair correlations, is quite well achieved for exponents γ close to 3. Smaller exponents γ yield ratios somewhat larger than 1, which, however, depend only weakly on ρ^{-1}. The reason for the larger ratios is presumably that these networks have larger fluctuations in the network connectivity structure. These topological fluctuations may lead to strong density fluctuations which are not captured by the current MF ansatz. For $\gamma>3$, the ratios become somewhat larger than 1 as well, as it is seen for $\gamma=3.5$. This behavior results from a segregation of the components, which is well known for lattices [8] and has already been observed by Gallos and Argyrakis [9] for networks with $\gamma>3$. That is, for networks with $\gamma>3$ the dynamics behaves as on lattices, which is as well reflected by the scaling relations from Eqs. (3) and (4) giving a linear in time density decay for networks with $\gamma>3$. Such segregation is not captured in our MF calculation of the pair correlations and is therefore out of range of its validity.

IV. CONCLUSIONS

This paper presents a detailed discussion of the $A+B\rightarrow\emptyset$ process on networks. We show analytically the existence of a "jamming" effect for this two component reaction and quantify it analytically with the correlations among unlike particles. The analysis can easily be generalized to multicomponent, pairwise processes and be used to derive a MF theory for a process where n particle types react pairwise with each other. Note, however, that the applicability is limited to cases where it is guaranteed that the particle densities are of the same order for all times. Otherwise, one component of the system with the largest density might cause a non-negligible jamming and could significantly slow down

the reaction. For the $A+B \rightarrow \emptyset$ process discussed here, we show that jamming is only important for vertices with small degree k and high densities. In the long-time, low-density limit we derive analytically that jamming vanishes for all vertices in the network, including the hubs. This conclusion is supported by numerical simulations and allows us to reason that the particle densities of the $A+B \rightarrow \emptyset$ process on scale-free, uncorrelated network show for each component the same scaling behavior as the one of the $A+A \rightarrow \emptyset$ process.

[1] R. Albert and A.-L. Barabási, Rev. Mod. Phys. **74**, 47 (2002).
[2] S. Dorogovtsev and J. Mendes, *Evolution of Networks* (Oxford University Press, Oxford, 2003).
[3] R. Pastor-Satorras and A. Vespignani, *Evolution and Structure of the Internet* (Cambridge University Press, Cambridge, 2004).
[4] R. Cohen, K. Erez, D. Avraham, and S. Havlin, Phys. Rev. Lett. **85**, 4626 (2000).
[5] M. Boguñá, R. Pastor-Satorras, and A. Vespignani, Phys. Rev. Lett. **90**, 028701 (2003).
[6] M. Boguñá, R. Pastor-Satorras, and A. Vespignani, in *Statistical Mechanics of Complex Networks*, edited by R. Pastor-Satorras, M. Rubi, and A. Diaz-Guilera, Vol. 625 of Lecture Notes in Physics (Springer Verlag, Berlin, 2003).
[7] D. Torney and H. McConnell, Proc. R. Soc. London, Ser. A **387**, 147 (1983).
[8] D. Toussaint and F. Wilczek, J. Chem. Phys. **78**, 2642 (1983).
[9] L. Gallos and P. Argyrakis, Phys. Rev. Lett. **92**, 138301 (2004).
[10] L. Gallos and P. Argyrakis, Phys. Rev. E **72**, 017101 (2005).
[11] M. Catanzaro, M. Boguñá, and R. Pastor-Satorras, Phys. Rev. E **71**, 056104 (2005).
[12] M. B. Hastings, Phys. Rev. Lett. **96**, 148701 (2006).
[13] N. V. Kampen, *Stochastic Processes in Physics and Chemistry* (Elsevier, Amsterdam, 1992).
[14] J. D. Noh and S. W. Kim, J. Korean Phys. Soc. **48**, S202 (2006).
[15] M. Molloy and B. Reed, Combinatorics, Probab. Comput. **7**, 295 (1998).
[16] M. Molloy and B. Reed, Random Struct. Algorithms **6**, 161 (1995).
[17] M. Catanzaro, M. Boguñá, and R. Pastor-Satorras, Phys. Rev. E **71**, 027103 (2005).
[18] M. Boguñá, R. Pastor-Satorras, and A. Vespignani, Eur. Phys. J. B **38**, 205 (2004).
[19] M. Newman, Phys. Rev. Lett. **89**, 208701 (2002).